Conference paper

Ariel A. Chialvo* and Lukas Vlcek

"Thought experiments" as dry-runs for "tough experiments": novel approaches to the hydration behavior of oxyanions

DOI 10.1515/pac-2015-1002

Abstract: We explore the deconvolution of correlations for the interpretation of the microstructural behavior of aqueous electrolytes according to the neutron diffraction with isotopic substitution (NDIS) approach toward the experimental determination of ion coordination numbers of systems involving oxyanions, in particular, sulfate anions. We discuss the alluded interplay in the title of this presentation, emphasized the expectations, and highlight the significance of tackling the challenging NDIS experiments. Specifically, we focus on the potential occurrence of $Ni^{2+}\cdots SO_4^{2-}$ pair formation, identify its signature, suggest novel ways either for the direct probe of the contact ion pair (CIP) strength and the subsequent correction of its effects on the measured coordination numbers, or for the determination of anion coordination numbers free of CIP contributions through the implementation of null-cation environments. For that purpose we perform simulations of $NiSO_4$ aqueous solutions at ambient conditions to generate the distribution functions required in the analysis (a) to identify the individual partial contributions to the total neutron-weighted distribution function, (b) to isolate and assess the contribution of $Ni^{2+}\cdots SO_4^{2-}$ pair formation, (c) to test the accuracy of the neutron diffraction with isotope substitution based coordination calculations and X-ray diffraction based assumptions, and (d) to describe the water coordination around both the sulfur and oxygen sites of the sulfate anion. We finally discuss the strength of this interplay on the basis of the inherent molecular simulation ability to provide all pair correlation functions that fully characterize the system microstructure and allows us to "reconstruct" the eventual NDIS output, i.e., to take an atomistic "peek" (e.g., see Figure 1) at the local environment around the isotopically-labeled species before any experiment is ever attempted, and ultimately, to test the accuracy of the "measured" NDIS-based coordination numbers against the actual values by the "direct" counting.

Keywords: computer simulation; electrolytes; hydration; ICSC-34; neutron diffraction; speciation.

Introduction

Oxyanions such as nitrates, carbonates, and sulfates are ubiquitous species in geochemical and industrial aqueous phase environments. In particular, the aqueous chemistry in the troposphere usually involves

Article note: A collection of invited papers based on presentations at the 34th International Conference on Solution Chemistry (ICSC-34), Prague, Czech Republic, 30th August – 3rd September 2015.

***Corresponding author: Ariel A. Chialvo,** Chemical Sciences Division, Geochemistry and Interfacial Sciences Group Oak Ridge National Laboratory, Oak Ridge, TN 37831-6110, USA, e-mail: ovlaich@gmail.com. http://orcid.org/0000-0002-6091-4563
Lukas Vlcek: Chemical Sciences Division, Geochemistry and Interfacial Sciences Group Oak Ridge National Laboratory, Oak Ridge, TN 37831-6110, USA; and Joint Institute for Computational Sciences Oak Ridge National Laboratory, Oak Ridge, TN 37831-6173, USA. http://orcid.org/0000-0003-4782-7702

Fig. 1: Atomistic peek of a representative contact $Ni^{2+}\cdots SO_4^{2-}$ pair in the 1.72 m $NiSO_4$ aqueous solution at ambient conditions.

hydrated nitrates resulting from the fast interaction between nitric acid and aerosol particles [1], while their interactions with sulfates are crucial in the homogeneous nucleation of ice particles [2]. Moreover, sulfate ions trigger changes of electrode activity in fuel cells [3], and are usually the signature of water pollution in fresh water environments [4]. Yet, despite its environmental and industrial relevance, little is understood about the hydration structure of the sulfate ion. As in the case of the hydration of nitrates [5, 6], sulfates exhibit weak – though not to the extent of the monovalent oxyanions – interactions with water whose pair correlation functions typically overlap those of the cation–water interactions [7–10]. Its weak hydration behavior, added to the ionic strength effect on the water dielectric permittivity, provides the opportunity to participate in cation-oxyanion $(M^{\nu+}\cdots SO_4^{2-})$ pairing as suggested by the wide range of experimental data of stability constants [11], and probes from electric conductivity [12–18], dielectric relaxation spectroscopy (DRS) [19–23], NMR [24], Raman [25–32], spectrophotometry [33–35], IR [36, 37], potentiometry [38–40], and osmometry [41, 42], even when the available XRD evidence [43–52] is still a matter of heated debate.

The current state of affairs is likely the result of a common factor behind the hydration of oxyanions manifested as the overlapping of several inter- and intra-atomic correlation peaks within the radial distance, $2.0 < r(\text{Å}) < 4.5$, including in this case the $H_2O\cdots SO_4^{2-}$ and the $M^{\nu+}\cdots SO_4^{2-}$ pair correlations. Considering that our ultimate goal is an improved understanding of the hydration behavior of the sulfate group, it is essential for us to be able to deconvolute the overlapping contributions prior to any interpretation of the coordinating environment. To achieve that goal we invoke a recently proposed NDIS approach based on the dual substitution on the oxyanions involving heavy- and null-aqueous environments [5], i.e., $^{nat}O_S/^{18}O_S$ and $^{nat}S/^{33}S$ for the current case of SO_4^{2-}, which provides a powerful means to settle the matter by detecting, isolating, and assessing directly the microstructural evidence regarding the presence of the $M^{\nu+}\cdots SO_4^{2-}$ pairing. This is made possible by the $^{nat}S/^{33}S$ scattering length difference, 1.89 fm, i.e., several times larger than the $^{nat}O_S/^{18}O_S$ corresponding difference, 0.204 fm; however, because the oxygen atomic concentration in the substituted SO_4^{2-} is obviously four times higher than that of the sulfur, the $^{nat}O_S/^{18}O_S$ contribution to the neutron weighted distribution functions will be comparable to (just about half) that of the $^{nat}S/^{33}S$ substitution.

Surprisingly, we are not aware of any NDIS data available in the literature for aqueous sulfates involving sulfur isotopic substitutions, despite the significant $^{nat}S/^{33}S$ neutron coherent scattering-length contrast [53]. The reason for this shortage might be traced back to the fact that the conventional combination of $^{nat}S/^{33}S$ and H/D substitutions provides complementary information for the solvation structure around sulfate anion, yet, neither addresses directly the near-neighbor coordination between the anion's oxygen and water. In fact, the few NDIS available experiments involving metal sulfates of which we are aware actually targeted the metal hydration behavior rather than the anion [54–57].

In this context, the main goal of the current work is to illustrate how a judicious interplay between statistical mechanics theory and molecular simulation can be used to test the accuracy and internal consistency of the NDIS approach for the determination of the aqueous coordination of the sulfate anion, i.e., as a dry-run for the actual experiments. For that purpose, we explore the eventual deconvolution of the contributions from $H_2O\cdots SO_4^{2-}$ correlations using neutron diffraction involving successive heavy- and null-aqueous solutions of $NiSO_4$ under $^{nat}S/^{33}S$ and $^{nat}O_S/^{18}O_S$ isotopic substitutions, i.e., $O_w\cdots O_S$, $H\cdots O_S$, $O_w\cdots S$, and $H\cdots S$, that would result in a full characterization of the first water coordination around SO_4^{2-}. In Section 2 we discuss the fundamentals underlying the novel first-order difference approach involving $^{nat}S/^{33}S$ and $^{nat}O_S/^{18}O_S$ substitutions in 1.72 m $NiSO_4$ aqueous solutions, where we manipulate the isotopic composition of the aqueous environment to allow the detection and isolation of the contact $M^{\nu+}\cdots SO_4^{2-}$ pair, as well as the definitive assessment of its strength and effect on the 'measured' anion-coordination numbers. After a brief description of the intermolecular potential models and the simulation methodology in Section 3, we discuss the microstructural behavior of the aqueous $NiSO_4$ and its characterization of the coordinating water environments according to the proposed interplay. Finally, we close the manuscript with a discussion and highlight the gist embedded in the title of this contribution.

Fundamentals

Neutron diffraction with isotopic substitution involving monoatomic ionic species has become a mature approach for the microstructural studies of aqueous electrolyte solutions [58–60] as long as the information from the NDIS raw data is corrected for the presence of ion-pairing [6, 61–64]. In contrast, NDIS experiments on aqueous electrolytes for the determination of the hydration microstructure of oxyanions involving dual $^{\alpha}Y/^{\beta}Y$ and $^{nat}O/^{18}O$ substitution are currently inexistent obviously due to the short time elapsed since Fischer et al.'s findings [65] regarding the more accurate assessment of the $^{nat}O/^{18}O$ difference of coherent scattering length, and the challenging nature of the NDIS experiments.

As we have recently highlighted it [5, 6], and due to the considerable experimental challenges behind the NDIS experiments involving null (i.e., neutron transparency to specific atoms) environment, it becomes extremely valuable to have available a molecular-based tool to conduct *a priori* analyses of the sought NDIS experiments. In this context, the interplay between statistical mechanics theory and molecular-based simulation affords a rigorous way to test unambiguously the accuracy of the approximations underlying the NDIS methodology. This is achievable because molecular simulation provides the full characterization of the system microstructure, i.e., not only the $s(s+1)/2$ pair correlation functions for a system involving s interacting sites (*vide infra*), but also the resulting NDIS output for any molecular model representing the system of interest. Precisely for this reason, the test of accuracy of the NDIS formalism becomes independent of the choice of the interaction potential models used in the simulation, yet, the reader might be understandably interested in knowing how realistic the used models are for the description of the aqueous electrolytes under investigation, an issue we have already addressed in great detail elsewhere [6].

The access to the $s(s+1)/2$ pair correlation functions by molecular simulation provides the unmatched opportunity to locate the relevant diffraction peaks, the presence of peak overlapping, and ultimately to facilitate the interpretation of the diffraction data. This is especially relevant for the study of oxyanion hydration, where it becomes practically impossible to extract any coordination information associated with the oxygen site of the oxyanion, unless we are able to discriminate it from the corresponding water–oxygen correlations. Therefore, in what follows we illustrate what we could expect to observe in a simulated NDIS experiment involving $^{nat}O/^{18}O$ and $^{nat}S/^{33}S$ in aqueous sulfate solutions, and discuss the implications on the accurate determination of water–sulfate coordination, where all microstructural details are known simultaneously with the corresponding first-order differences of the neutron weighted distribution functions. This feature allows the unambiguous identification of peak overlapping between pair correlation functions, and consequently, the isolation of specific pair correlation peaks for the assessment of meaningful species coordination as well as the opportunity to test conjectured behaviors underlying the potential occurrence of ion-pairing and its effect in the interpretation of the NDIS raw data [62, 66].

Neutron diffraction with dual $^{nat}S/^{33}S$ and $^{nat}O_S/^{18}O_S$ isotopic substitution

Here we examine the link between the measured quantities and the targeted microstructures (e.g., ion coordination environment), and identify the (frequently dismissed) problems underlying the meaningful interpretation of the experimental evidence, such as the unavoidable peak overlapping as the signature of ion-pair formation [62, 66]. The starting point is the portion of the neutron scattering differential cross section of the aqueous sample, $d\sigma/d\Omega$, that comprises the desired information on the microstructure, i.e., the total structure factor $F(k)$ defined as [67],

$$F(k) = \sum_{i \le j} (2 - \delta_{ij}) c_i c_j b_i b_j (S_{ij}(k) - 1) \tag{1}$$

where $k = (4\pi/\lambda)\sin(\theta/2)$, λ of the incident neutron wavelength, while θ, c_i and b_i denote the scattering angle, the atomic fraction and the coherent neutron scattering length of the atomic species i, respectively. Obviously $F(k)$ is a linear combination of the partial structure factor $S_{ij}(k)$ describing the correlation between atoms of types i and j, i.e.,

$$S_{ij}(k) = 1 + (4\pi\rho/k)\int_0^\infty [g_{ij}(r) - 1] r \sin(kr)\, dr \tag{2}$$

where ρ and $g_{ij}(r)$ are the atomic number density of the solution and the corresponding radial pair distribution function for ij-pair interactions. For most practical purposes we prefer dealing with the total (real space neutron-weighted) pair correlation function $G(r)$ rather than $F(k)$, i.e., its Fourier transform,

$$G(r) = \sum_{i \le j} (2 - \delta_{ij}) c_i c_j b_i b_j (g_{ij}(r) - 1) \tag{3}$$

Considering that a simple $M^{\nu+}XO_x^{\nu-}$ aqueous solution of the oxyanion $XO_x^{\nu-}$ and the cation $M^{\nu+}$ comprises s scattering species then, in principle, there are $s(s+1)/2$ independent radial distribution functions $g_{ij}(r)$ defining the system microstructure. Consequently, any attempt to determine the ion coordination would in principle require the same number of experiments (i.e., involving different isotopic compositions) to extract the full set of $g_{ij}(r)$ [68]. Obviously, this approach would be infeasible because *inter alia* the overwhelming contribution from water-water correlation functions [either $g_{OH}(r)$ and $g_{HH}(r)$ or $g_{OD}(r)$ and $g_{DD}(r)$] to $G(r)$ will hamper any attempt to extract relevant information about the local aqueous environment around the ions and the analysis of ion pair formation, and the fact that we need only the profile of a few correlation functions, over a limited $[r_L, r_U]$ radial interval, associated with the targeted ion environment.

The reasonable way to circumvent this shortcoming is through the cancelation of the undesired correlations via the implementation of the first-order difference scheme [69], i.e., comprising two diffraction experiments involving a pair of identical solutions except for the isotopic states of the species (labeled α or β) under study. Then, the ion coordination can be determined by the integration of the resulting first-order difference within the radial interval $[r_L, r_U]$ where the sought ion-water correlation occurs and exhibits no peak overlapping (*vide infra*). Specifically, the cancelation of contributions from the solvent–solvent and solvent–(non-substituted) solute species interactions in the first-order difference scheme for the study of the coordination around the SO_4^{2-} anion might result in the following expressions,

$$\Delta G_S^{\text{solv,norm}}(r) = [A_S g_{O_W S}(r) + B_S g_{DS}(r) + C_S g_{HS}(r) + D_S g_{MS}(r) + E_S g_{SS}(r) + F_S g_{O_S S}(r)] / \Sigma_S^{\text{solv}} \tag{4}$$

with $\Sigma_S^{\text{solv}} = A_S + B_S + C_S + D_S + E_S + F_S$ under the $^{nat}S/^{33}S$ substitution, and

$$\Delta G_O^{\text{solv,norm}}(r) = [A_O g_{O_W O_S}(r) + B_O g_{DO_S}(r) + C_O g_{HO_S}(r) + D_O g_{MO_S}(r) + E_O g_{O_S O_S}(r) + F_O g_{SO_S}(r)] / \Sigma_O^{\text{solv}} \tag{5}$$

with $\Sigma_O^{solv} = A_O + B_O + C_O + D_O + E_O + F_O$ under the $^{nat}O_S/^{18}O_S$ substitution, where we have explicitly identified the two distinct isotopic variants of the oxygen species, i.e., O_W for the natural oxygen isotope in water and O_S as the sulfate oxygen undergoing the isotopic substitution. Note that in eqs. (4)–(5) we have also differentiated explicitly the hydrogen isotopes of the water as $H \equiv {}^1H$ and $D \equiv {}^2H$ so that the solvent (solv) environment can be represented by light-, heavy-, or null-aqueous environments, i.e., for which $B_S = B_O = 0$, $C_S = C_O = 0$, or $B_S + C_S = B_O + C_O = 0$, respectively. Moreover, the prefactors of the six contributions in eqs. (4)–(5) are given by $c_i c_j b_j [\, b_i^{\alpha}(2 - \delta_{ji^{\alpha}}) - b_i^{\beta}(2 - \delta_{ji^{\beta}})]$, where we emphasize the isotopic dependence of the corresponding coherent neutron scattering lengths (b_i^l with $l = \alpha, \beta$) for the isotopic species, and invoke Kronecker delta δ_{ji^l}.

A further manipulation of the system environment could be achieved by making the M-cation transparent to the neutrons by means of the so-called null M-cation (*nM*) environment, involving the $^{\alpha}M/^{\beta}M$ isotopic substitution at an isotopic composition $c_{\alpha_M}/c_{\beta_M} = -(b_{\beta_M}/b_{\alpha_M})$ that makes $D_S = D_O = 0$, so that eqs. (4)–(5) reduce to the following working expressions,

$$\Delta G_{S,nM}^{hw,norm}(r) = [\, A_S g_{O_W S}(r) + B_S g_{DS}(r) + E_S g_{SS}(r) + F_S g_{O_S S}(r)] \,/\, \Sigma_{S,nM}^{hw} \tag{6}$$

with $\Sigma_{S,nM}^{hw} = A_S + B_S + E_S + F_S$ and,

$$\Delta G_{O,nM}^{hw,norm}(r) = [\, A_O g_{O_W O_S}(r) + B_O g_{DO_S}(r) + E_O g_{O_S O_S}(r) + F_O g_{SO_S}(r)] \,/\, \Sigma_{O,nM}^{hw} \tag{7}$$

with $\Sigma_{O,nM}^{hw} = A_O + B_O + E_O + F_O$. The goal behind the use of the null-cation environment is to erase any contribution form the $M^{\nu+}\cdots SO_4^{2-}$ pair interactions, i.e., $M\cdots O_S$ and $M\cdots S$ whose correlation peaks usually overlap with the hydration relevant anion interactions such as $H\cdots O_S$ and $H\cdots S$ (*vide infra*, Figs. 2 and 3). In other words, by eliminating the ion-pair contributions from the onset, we should be able to avoid the CIP correction of the corresponding 'measured' coordination numbers, i.e., $\overline{n}_S^D(r_s, \text{measured})$ and $\overline{n}_{O_S}^D(r_s, \text{measured})$ as already discussed and illustrated elsewhere for the alkali and alkaline-earth halides counterparts [6, 62, 66].

Typically, assuming that there are additional contributions (other than $g_{DS}(r)$) to $\Delta G_S^{solv,norm}(r)$ from other correlations in the $[r_L, r_U]$ radial interval, after invoking the statistical mechanical definition of coordination number, i.e.,

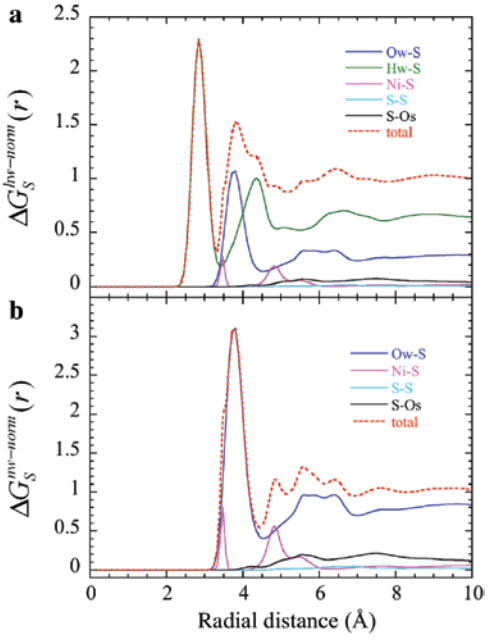

Fig. 2: Normalized first-order difference of neutron weighted distribution functions for the 1.72 m $NiSO_4$ in heavy- and null-water solution at ambient conditions under $^{nat}S/^{33}S$ substitution.

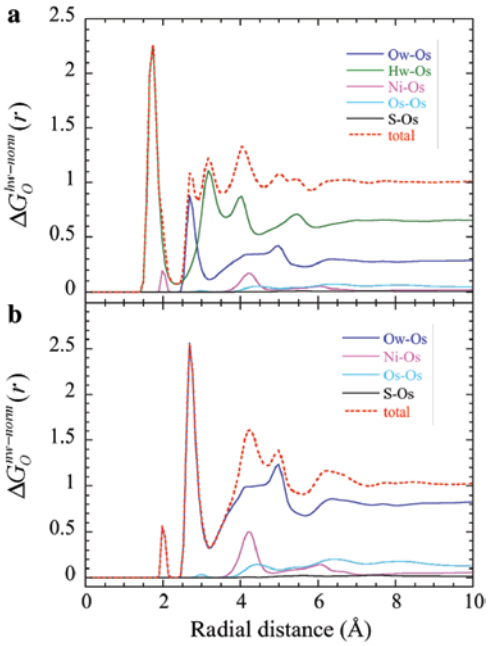

Fig. 3: Normalized first-order difference of neutron weighted distribution functions for the 1.72 m $NiSO_4$ in heavy- and null-water solution at ambient conditions under $^{nat}O/^{18}O$ substitution.

$$\overline{n}_I^{\beta}(r_s) = 4\pi\rho_{\beta}\int_0^{r_s} g_{\beta I}(r)r^2dr \tag{8}$$

where β = H, O and r_s typically locates the first valley of the radial distribution function $g_{\beta I}(r)$, we have that the coordination of water around the sulfate's sulfur site becomes,

$$\overline{n}_S^{D}(r_s) = (4\pi\rho_D\Sigma_S^{hw}/B_S^{hw})\int_{r_L}^{r_U}\Delta G_S^{hw,\mathrm{norm}}(r)r^2dr \tag{9}$$

and,

$$\overline{n}_S^{O_W}(r_s) = (4\pi\rho_{O_W}\Sigma_S^{hw}/A_S^{hw})\int_{r_L}^{r_U}\Delta G_S^{hw,\mathrm{norm}}(r)r^2dr \tag{10}$$

while the result corresponding to the sulfate's oxygen site reads,

$$\overline{n}_{O_S}^{D}(r_s) = (4\pi\rho_D\Sigma_O^{hw}/B_O^{hw})\int_{r_L}^{r_U}\Delta G_O^{hw,\mathrm{norm}}(r)r^2dr \tag{11}$$

and,

$$\overline{n}_{O_S}^{O_W}(r_s) = (4\pi\rho_{O_W}\Sigma_O^{hw}/A_O^{hw})\int_{r_L}^{r_U}\Delta G_O^{hw,\mathrm{norm}}(r)r^2dr \tag{12}$$

Interaction potential models and molecular simulation methodology

For the analysis of the hydration behavior of the aqueous $NiSO_4$ and to illustrate the interplay as well as issues discussed above, we performed isochoric–isothermal molecular dynamics simulations at ambient conditions. For that purpose we have chosen simple but reliable intermolecular potential models including the rigid SPC/E water [70], and the Wallen et al. [71], and the five-sites rigid tetrahedral Cannon et al. [72] for the nickel and sulfate ions, respectively. All these potential models involve Lennard–Jones models, with the

unlike pair interactions described by the Lorentz–Berthelot combining rules, and site-site electrostatic interactions according to the force field collected in Table 1.

All simulations involved $N_W = 1986$ water molecules and $N_{\text{ions}} = 2N_{\text{Ni}} = 124$ ions and were carried out according to our own implementation of a Nosé–Poincare algorithm [73, 74] for the integration of the Newton–Euler equations of motion within a cubic simulation box of dimension L under 3D periodic boundary conditions. The initial configuration was generated by the *Packmol* utility [75] and equilibrated by at least 1.0 ns, followed by production runs of 4.0 ns, using an integration time-step of 2.0 fs, during which the microstructural information was collected. All Lennard–Jones interactions were truncated at a cut-off radius $\min(r_c \approx 3.5\sigma_{\text{SPCE}}, r_c = L/2)$, while the electrostatic interactions were handled by an Ewald summation whose convergence parameters were chosen to assure an error smaller than $5 \times 10^{-5}\varepsilon_{\text{SPCE}}$ for both the real and reciprocal spaces [76].

Microstructural results

From the ten simulated pair correlation functions we determined the first-order differences of neutron-weighted radial distribution functions, for the heavy-water – $\Delta G_S^{hw,\text{norm}}(r)$ and $\Delta G_O^{hw,\text{norm}}(r)$ – and the null-water – $\Delta G_S^{nw,\text{norm}}(r)$ and $\Delta G_O^{nw,\text{norm}}(r)$ – as well as the null-nickel – $\Delta G_{S,n\text{Ni}}^{hw,\text{norm}}(r)$ and $\Delta G_{O,n\text{Ni}}^{hw,\text{norm}}(r)$ – for the two isotopic substitutions in SO_4^{-2} that will be later used for the estimation of the corresponding coordination numbers as well as the analysis of ion-pair formation.

In Table 2 we collect the values of the coherent scattering lengths used in the study, which were taken from the available literature. The first-order differences $\Delta G_S^{\text{solv,norm}}(r)$ and $\Delta G_O^{\text{solv,norm}}(r)$ for heavy- and null-water, as well as the contributions from each pair interactions are plotted in Figs. 2ab–3ab. The coefficients of the first-order differences, eqs. (4)–(5) are collected in Table 3 and 4, where the contrasting magnitudes of these coefficients, i.e., $A_\ell, B_\ell >> D_\ell, E_\ell, F_\ell$ and $A_S, B_S > A_O, B_O$ highlight the facts that, as in the case of aqueous nitrates, the two most relevant contributions to $\Delta G_\ell^{\text{solv,norm}}(r)$ come from the nearest pair interactions between the ℓ– substituted species and water, and the fact that coherent scattering contrast for the $^{\text{nat}}S/^{33}S$ substitution is larger than that for the $^{\text{nat}}O_S/^{18}O_S$ substitution.

Table 1: Potential parameters for the aqueous $NiSO_4$ model solutions.[c]

ii-Interaction	ε_{ii}/k(K)[a]	σ_{ii}(Å)[b]	q_i(e)	Refs.
Ni···Ni	50.34	2.050	2.0	[71]
O_S···O_S	30.09	3.150	−1.100	[72]
S···S	125.7	3.550	2.400	[72]
O_W···O_W	125.7	3.166	−0.8476	[70]
H···H	–	–	0.4238	[70]

[a] $\varepsilon_{ij} = \sqrt{\varepsilon_{ii}\varepsilon_{jj}}$; [b] $\sigma_{ij} = 0.5(\sigma_{ii} + \sigma_{jj})$; [c] bond-length $\ell_{SO} = 1.49$ Å [72].

Table 2: Coherent neutron scattering lengths for aqueous $NiSO_4$.

Species	b_{coh}(fm)	Refs.
$^{\text{nat}}S$	2.847	[53]
^{33}S	4.74	[53]
^{1}H	−3.74	[53]
^{2}H	6.67	[53]
$^{\text{nat}}O$	5.805	[53]
^{18}O	6.009	[65]
$^{\text{nat}}Ni$	10.30	[53]
^{62}Ni	−8.7	[53]

Table 3: Coefficients of the first-order difference of weighted distributions for the $^{nat}S/^{33}S$ substitution in 1.72 m $NiSO_4$ heavy- and null-aqueous solutions.

Coefficient[a]	Heavy-water	Null-water
A_S	6.945079E-02	6.945079E-02
B_S	0.1595992	5.732689E-02
C_S	0.0	−5.732689E-02
D_S	3.970990E-03	3.970990E-03
E_S	1.462520E-03	1.462520E-03
F_S	8.952077E-03	8.952077E-03
Σ_N^{solv}	0.2434356	8.383637E-02

[a]In fm^2 units.

Table 4: Coefficients of the first-order difference of weighted distributions for the $^{nat}O_S/^{18}O_S$ substitution in 1.72 m $NiSO_4$ heavy- and null-aqueous solutions.

Coefficient[a]	Heavy-water	Null-water
A_O	2.993758E-02	2.993758E-02
B_O	6.879714E-02	2.472620E-02
C_O	0.0	−2.472620E-02
D_O	1.711742E-03	1.711742E-03
E_O	3.926700E-03	3.926700E-03
F_O	4.731388E-04	4.731388E-04
Σ_O^{solv}	0.1048463	3.604916E-02

[a]In fm^2 units.

The main features of $\Delta G_S^{hw,\mathrm{norm}}(r)$, Fig. 2a, are rather similar to those of the nitrate counterparts, i.e., two prominent peaks at ~2.85 Å and ~3.80 Å corresponding to the nearest D···S interactions, and the combination of contributions from the second nearest D···S, the O_w···S, as well as the contribution from the contact Ni···S pair interactions. Moreover, the occurrence of O_w···S, Ni···S, and D···S correlation peaks within $3.2 \le r(\text{Å}) \le 5.0$, hinders the determination of the second D···S coordination by integration of the second peak of $\Delta G_S^{hw,\mathrm{norm}}(r)$, a common feature shared by most aqueous oxyanions (*vide supra*).

However, the first peak of $\Delta G_S^{hw,\mathrm{norm}}(r)$, Fig. 2a, comprises almost exclusively the contribution from the first peak of the corresponding $g_{DS}(r)$, with two small contributions from the O_w···S and the contact Ni···S pair interactions. Consequently, the outcome for the first coordination number $n_D^S(r)$ based on the integration of $\Delta G_S^{hw,\mathrm{norm}}(r)$, eq. (9), could be slightly smaller than the true one, eq. (8) and Table 5, and highlights the effect of additional contributions [other than $g_{DS}(r)$] to $\Delta G_S^{hw,\mathrm{norm}}(r)$ from the overlapping with other correlations in the $[r_L, r_U]$ radial interval.

The first peak of $\Delta G_S^{nw,\mathrm{norm}}(r)$, Fig. 2b, is centered at $r \approx 3.8$ Å and comprises a major contribution from O_w···S interactions that fully overlap with the contact Ni···S pair configurations. Consequently, the conventional determination of the water-oxygen coordination around the sulfur site of the sulfate group, i.e.,

$$\overline{n}_S^{O_w}(r_s) = (4\pi\rho_{O_w}\Sigma_S^{nw} / A_S^{nw})\int_{r_L}^{r_U} \Delta G_S^{nw,\mathrm{norm}}(r) r^2 dr \tag{13}$$

will experience the same problem as that for $\overline{n}_S^D(r_s)$ from $\Delta G_S^{hw,\mathrm{norm}}(r)$, eq. 9, due to the presence of two smaller overlapping contributions from the contact Ni···S and the O_S···S pair correlation peaks (Table 5).

Note that $\overline{n}_{O_s}^{\mathrm{Ni}}(\mathrm{CIP}) \simeq \overline{n}_S^{\mathrm{Ni}}(\mathrm{CIP})$ rather than what has been usually assumed in the interpretation of XRD based on the nearest intra-molecular coordination [46], i.e., $\overline{n}_{O_s}^{\mathrm{Ni}}(\mathrm{CIP}) \simeq \overline{n}_S^{\mathrm{Ni}}(\mathrm{CIP})/4$, resulting from the different sizes of the coordination shells, $r_u = 2.2$ Å for $\overline{n}_{O_s}^{\mathrm{Ni}}(\mathrm{CIP})$ and $r_u = 3.37$ Å for $\overline{n}_S^{\mathrm{Ni}}(\mathrm{CIP})$.

Table 5: First water coordination of the sulfate ion in 1.72 m $NiSO_4$ heavy- and null-aqueous solutions according to the direct and the NDIS-based expressions.

α–β interactions	Direct integral (r_u)[c]	NDIS integral (r_u)[d]
$O_W\cdots S$	14.1(4.51 Å)	14.7(4.43 Å)[b]
$D\cdots S$	11.6(3.40 Å)	11.4(3.32 Å)[a]
$O_W\cdots O_S$	3.2(3.16 Å)	3.6(3.24 Å)[b]
$D\cdots O_S$	2.8(2.37 Å)	3.1(2.37 Å)[a]
$Ni\cdots S$	0.4(3.37 Å)	–
$O_S\cdots Ni$	0.4(2.20 Å)	0.4(2.20 Å)[b]

[a]Heavy-water; [b]null-water; [c] $\overline{n}^{\alpha}_{\beta}(r_s)=4\pi\rho_{\alpha}\int_0^{r_s} g_{\alpha\beta}(r)r^2dr$; [d] $\overline{n}^{\alpha}_{\beta}(r_s)=(4\pi\rho_{\alpha}\Sigma^{solv}_{\beta}/I^{solv}_{\alpha\beta})\int_0^{r_s}\Delta G^{solv,norm}_{\beta}(r)r^2dr$ with solv = (*hw*, *nw*) and $I^{solv}_{\alpha\beta}=(A^{solv}_{\beta}\ if\alpha=O_w;\ B^{solv}_{\beta}\ if\alpha=D)$.

In Fig. 3a–b we display the corresponding first-order differences $\Delta G^{hw,norm}_{O}(r)$ and $\Delta G^{nw,norm}_{O}(r)$ counterparts to Fig. 2a–b, where we immediately note that $\Delta G^{hw,norm}_{O}(r)$ exhibits a well defined first peak associated with the $D\cdots O_S$ correlations centered at $r\approx 1.75$ Å similar to the $D\cdots O_W$ peak for pure water [77], yet, it overlaps completely the contribution from the contact $Ni\cdots O_S$ pair peak. Beyond the first peak, $\Delta G^{hw,norm}_{O}(r)$ presents a less defined multi-peak region resulting from the overlapping of the second $D\cdots O_S$ coordination, the solvent-shared $Ni\cdots O_S$ pair, and the two $O_W\cdots O_S$ correlation peaks. As a first approximation we can ignore the small contact $Ni\cdots O_S$ pair contribution to the first peak of $\Delta G^{hw,norm}_{O}(r)$, then its integral will provide an adequate estimate for the first coordination $\overline{n}^{D}_{O_s}(r_s)$ as clearly depicted in Table 5. This number can then be corrected as soon as we determine the first coordination for the $Ni\cdots O_S$ interactions. For that purpose, we turn our attention to the behavior of $\Delta G^{nw,norm}_{O}(r)$, Fig. 3b, where the first peak describes the nearest $Ni\cdots O_S$ interactions, which by integration of $\Delta G^{nw,norm}_{O}(r)$ up to a distance $r\approx 2.2$ Å, provides an adequate estimation of $\overline{n}^{Ni}_{O_s}(r_s)$.

$$\overline{n}^{D}_{O_s}(r_s,\text{ measured})=(4\pi\rho_D/B_O)\int_{r_L}^{r_U}(B_O g_{DO_s}(r)+D_O g_{OsNi}(r))r^2dr=\overline{n}^{D}_{O_s}(r_s)+\underbrace{(4\pi\rho_D D_O/B_O)\int_{r_L}^{r_U} g_{OsNi}(r)r^2dr}_{\text{CIP contribution}} \quad (14)$$

Then the actual $\overline{n}^{D}_{O_s}(r_s)$ can be assessed by subtracting the CIP– contribution written explicitly as follows,

$$(4\pi\rho_{Ni}b_{Ni}/b_D)\int_{r_L}^{r_U} g_{OsNi}(r)r^2dr=\overline{n}^{Ni}_{O_s}(r_s)(b_{Ni}/b_D) \quad (15)$$

from eq. (12) to attain,

$$\overline{n}^{D}_{O_s}(r_s)=\overline{n}^{D}_{O_s}(r_s,\text{ measured})-\overline{n}^{Ni}_{O_s}(\text{CIP})(b_{Ni}/b_D) \quad (16)$$

Obviously, according to Figs. 2 and 3, there are no chances of assessing the $\overline{n}^{Ni}_{S}(\text{CIP})$ and its contribution to the $\overline{n}^{O_w}_{S}(r_s,\text{ measured})$ for the subsequent correction according to eq. (16) counterpart, even if we could derive the corresponding expression, i.e.,

$$\begin{aligned}\overline{n}^{O_w}_{S}(r_s,\text{ measured})&=(4\pi\rho_{O_w}/A_S)\int_{r_L}^{r_U}(A_S g_{OwS}(r)+D_S g_{NiS}(r))r^2dr\\&=\overline{n}^{O_w}_{S}(r_s)+\underbrace{(4\pi\rho_{O_w}D_S/A_S)\int_{r_L}^{r_U} g_{NiS}(r)r^2dr}_{\text{CIP contribution}}\end{aligned} \quad (17)$$

so that,

$$\overline{n}^{O_w}_{S}(r_s)=\overline{n}^{O_w}_{S}(r_s,\text{ measured})-\overline{n}^{O_w}_{S}(\text{CIP})(b_{Ni}/b_{O_w}) \quad (18)$$

However, we still have another source of information to characterize further the water coordination of the sulfate anion, i.e., the null-nickel venue through the manipulation of the isotopic composition of the cation. Under this null-nickel environment the relevant distribution functions $\Delta G^{hw,\mathrm{norm}}_{S,n\mathrm{Ni}}(r)$ and $\Delta G^{hw,\mathrm{norm}}_{O,n\mathrm{Ni}}(r)$, given by eqs. (6)–(7) and illustrated in Fig. 4a–b, indicate that the absence of any type of Ni···O_S or Ni···S pairing. Consequently, we can extract the water-hydrogen coordination of the sulfur and oxygen sites of the sulfate anion with no interference from the potential CIP configurations, i.e.,

$$\overline{n}^{D}_{S}(r_s) = (4\pi\rho_D \Sigma^{hw}_{S,n\mathrm{Ni}} / B_S)\int_0^{r_s} \Delta G^{hw,\mathrm{norm}}_{S,n\mathrm{Ni}}(r) r^2 dr \tag{19}$$

and,

$$\overline{n}^{D}_{O_s}(r_s) = (4\pi\rho_D \Sigma^{hw}_{O,n\mathrm{Ni}} / B_O)\int_0^{r_s} \Delta G^{hw,\mathrm{norm}}_{O,n\mathrm{Ni}}(r) r^2 dr \tag{20}$$

Note that due to the absence of any contact (anion site-cation) pair corrections, the coordination number determined by eq. (19) will provide a test of consistency for the calculations involving eq. (16). As an illustration of the issue, in Table 6 we made the comparison between the reference coordination numbers given by their statistical mechanical definition, i.e., eq. (8).

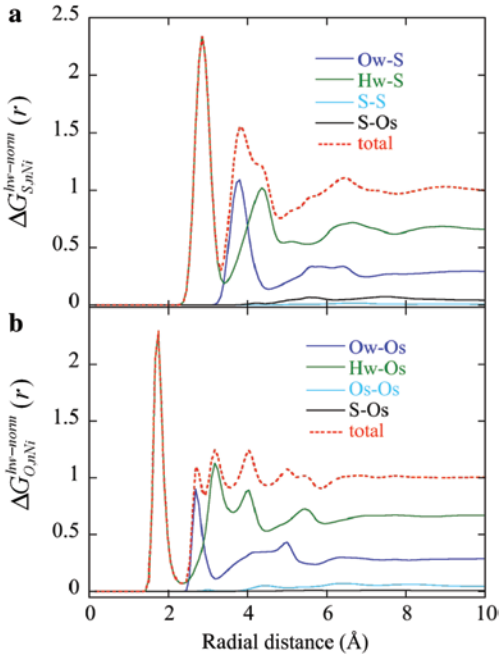

Fig. 4: Normalized first-order difference of neutron weighted distribution functions for the 1.72 m $NiSO_4$ in heavy-water null-Ni solution at ambient conditions under either $^{nat}O/^{18}O$ or $^{nat}S/^{33}S$ substitution.

Table 6: First water coordination of the sulfate ion in 1.72 m $NiSO_4$ aqueous solutions from integrals over $\Delta G^{\mathrm{solv,norm}}_{S}(r)$, $\Delta G^{\mathrm{hw,norm}}_{S,n\mathrm{Ni}}(r)$, $\Delta G^{\mathrm{solv,norm}}_{O}(r)$, and $\Delta G^{\mathrm{hw,norm}}_{O,n\mathrm{Ni}}(r)$.

α–β Interactions	Direct integral(r_u)[b]	NDIS integral (r_u)[a]	NDIS integral (r_u)
D···S	11.6(3.40 Å)	11.4(3.32 Å)	11.4(3.32 Å)[c]
D···O_S	2.8(2.37 Å)	3.1(2.37 Å)	2.8(3.7 Å)[d]

[a] $\overline{n}^{D}_{X}(r_s) = \overline{n}^{D}_{X}(\mathrm{measured}) - \overline{n}^{\mathrm{Ni}}_{X}(r_s)(b_{\mathrm{Ni}}/b_D)$ where $X = [O_S, S]$, $\overline{n}^{\mathrm{Ni}}_{O_s}(\mathrm{CIP}) \cong 0.4$ (Table 5), $\overline{n}^{\mathrm{Ni}}_{S}(\mathrm{CIP}) \cong 0.4$ (Table 5); [b]from eq. (8); [c]eq. (19); [d]eq. (20).

Up to this point we have presented the tools and illustrated their use not only to detect the presence of (CIP) $M^{\nu+}\cdots SO_4^{2-}$ but also to isolate it, and finally to estimate a representative coordination number. Yet, we have not addressed the extent of such an ion-pair association, i.e., the degree of $M^{\nu+}\cdots SO_4^{2-}$ pair and its link to an association constant, rather than a CIP coordination number $\bar{n}_X^M(r_L, r_U)$ with $X=[O_S, S]$, as well as the participation of CIP, SShIP, and SSIP configurations according to the Eigen-Tamm classification [78]. For that purpose we invoke a somewhat less-known rigorous formalism to make such a connection [6, 79, 80].

The degree of either $M^{\nu+}\cdots S[O_4^{2-}]$ or $M^{\nu+}\cdots O[SO_3^{2-}]$ pair association α_{-+} can be expressed in terms of the ion-pair distribution function $G_{-+}(r)$ related to the corresponding pair correlation function $g_{-+}(r)$) as an integral equation, i.e.,

$$G_{-+}(r) = 4\pi\rho_+ g_{-+}(r) r^2 P_-(r) P_+(r) \tag{21}$$

where $P_-(r)$ ($P_+(r)$) denotes the probability that either $S[O_4^{2-}]$ or $O[SO_3^{2-}]$ separated by a distance r from an $M^{\nu+}$ (either $S[O_4^{2-}]$ or $O[SO_3^{2-}]$) does not engage in an ion pair with any other ion of the opposite charge, i.e., $P_-(r) = 1 - \int_0^r G_{-+}(s)ds$ and $P_+(r) = 1 - \int_0^r G_{+-}(s)ds$. Typically, the solution of this integral equation is analytical and involves the obvious conservation of species and electroneutrality boundary conditions (for more details on the resulting expressions see Refs. [6, 79, 80]). Then, the degree of either $M^{\nu+}\cdots S[O_4^{2-}]$ or $M^{\nu+}\cdots O[SO_3^{2-}]$ pair association reads,

$$\alpha_{-+}(d_{-+}) = \int_0^{d_{-+}} G_{-+}(r)dr \tag{22}$$

under the condition that, in the thermodynamic limit, $\lim_{d_{-+}\to\infty} \alpha_{-+}(d_{-+}) = 1.0$, where d_{-+} typically denotes the largest distance within which the pairs are counted, such as the location of the first (for contact ion pairs) or second valley (for contact plus solvent-shared ion pairs) of $g_{-+}(r)$.

In Fig. 5a–b we display the $Ni^{+2}\cdots S[O_4^{2-}]$ radial distribution functions $g_{-+}(r)$, as well as their corresponding ion-pair radial distribution functions $G_{-+}(r)$ and degree of ion-pair association $\alpha_{-+}(r)$ for the 1.72 m $NiSO_4$ aqueous solution at ambient conditions, where we should highlight the significant difference in the magnitude between $G_{-+}(r)$ and $g_{-+}(r)$ functions, and the obvious correspondence between

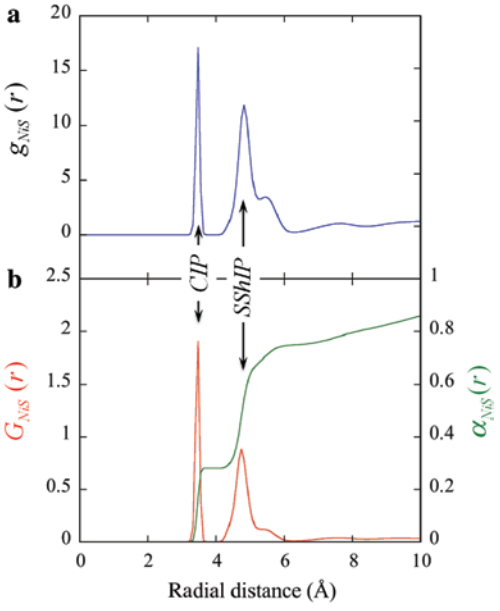

Fig. 5: Radial pair distribution function $g_{NiS}(r)$, the corresponding Pourier-deLap $Ni^{+2}\cdots S[O_4^{2-}]$ pair distribution function and the resulting degree of pair association for the 1.72 m $NiSO_4$ aqueous solution at ambient conditions.

their two main peaks associated with the CIP and SShIP configurations. Moreover, note that even at this low sulfate concentration the system exhibits a significant $Ni^{+2}\cdots S[O_4^{2-}]$ pair association characterized by $\alpha(\text{CIP}) \cong 0.28$, with $\alpha(\text{CIP}+\text{SShIP}) \geq 0.75$. The last value is in remarkable agreement with the reported value of $\alpha(1.6 \leq m \leq 1.8) \approx 0.69$ for ambient $NiSO_4$ aqueous solutions in Table 5 of Ref. [81].

Discussion and final remarks

We have described the fundamentals underlying the interpretation of microstructural behavior of aqueous electrolytes according to the NDIS approach toward the experimental determination of ion coordination numbers of systems involving sulfate anions. We discussed the 'philosophy' motivating the interplay alluded to in the title of this presentation, and emphasized the expectations as well as significance of tackling the challenging NDIS experiments. Specifically, we highlighted the potential occurrence of $M^{\nu+}\cdots SO_4^{2-}$ pair formation with both anion interaction sites, a frequently overlooked hydration phenomenon, identified its signature in the neutron-weighted distribution functions, suggested novel ways for either the direct probe of the CIP strength for the subsequent correction of its effects on the experimentally measured coordination numbers, or the determination of anion coordination numbers free of CIP contributions through the implementation of null-cation environments.

We must emphasize that this interplay becomes a formidable asset after recognizing the inherent molecular simulation ability to provide all pair correlation functions that fully characterize the system microstructure and allows us to "reconstruct" the eventual NDIS output, i.e., to take an atomistic "peek" at the local environment around the isotopically-labeled species before any experiment is ever attempted, and ultimately, to test the accuracy of the "measured" NDIS-based coordination numbers against the actual values by the "direct" counting. In addition, the isotopic differentiation between O_W and O_S in eqs. (4)–(7) provides a handy way to check the consistency of the experimental raw data sets according to the natural constraint given by the intra-molecular coordination $n_S^{O_S}(\ell_{SO}) = 4$, where ℓ_{SO} is the intra-molecular bond-length. For that purpose we introduce the definition of intra-coordination and invoke un-normalized eq. (4), i.e.,

$$\begin{aligned} n_S^{O_S}(\ell_{SO}) &= 4\pi\rho_{O_S}\int_{\ell_{SO}-\delta}^{\ell_{SO}+\delta} g_{SO_S}(r)r^2dr \\ &= (4\pi\rho_{O_S}/F_S)\int_{\ell_{SO}-\delta}^{\ell_{SO}+\delta}[\Delta G_S^{\text{solv}}(r)+\Sigma_S^{\text{solv}}]r^2dr \end{aligned} \tag{23}$$

where $\Sigma_S^{\text{solv}} = A_S + B_S + C_S + D_S + E_S + F_S \ldots$ Likewise, from eq. (5) we have that,

$$\begin{aligned} n_{O_S}^{S}(\ell_{SO}) &= 4\pi\rho_{S}\int_{\ell_{SO}-\delta}^{\ell_{SO}+\delta} g_{O_SS}(r)r^2dr \\ &= (4\pi\rho_{S}/F_O)\int_{\ell_{SO}-\delta}^{\ell_{SO}+\delta}[\Delta G_O^{\text{solv}}(r)+\Sigma_O^{\text{solv}}]r^2dr \end{aligned} \tag{24}$$

with $\Sigma_O^{\text{solv}} = A_O + B_O + C_O + D_O + E_O + F_O$, where the parameter δ describes the spread of the distribution of the intra-molecular bond length ℓ_{SO} in the real system. Obviously, for a model system with rigid geometry for the sulfate anion, as for Cannon et al. [72], the bond-length distributions in eqs. (23)–(24) become delta functions, i.e., the constraint is satisfied by construction, i.e.,

$$\begin{aligned} n_{O_S}^{S}(\ell_{SO}) &= 4\pi\rho_{S}\int g_{SO_S}(r)r^2\delta(r-\ell_{SO})dr \\ &= \pi\rho_{O_S}\int g_{O_SS}(r)r^2\delta(r-\ell_{SO})dr = n_S^{O_S}(\ell_{SO})\big/4 \end{aligned} \tag{25}$$

where $g_{SO_S}(r) = g_{OS_S(r)}$. Note that the equality of the two lines in eqs. (23)–(25) is guaranteed as long as there is no overlapping of peaks within the range of intra-molecular interactions, i.e., the self-consistency of $\Delta G_S^{\text{solv}}(r)$ and $\Delta G_O^{\text{solv}}(r)$ will mean that,

$$c_{O_S} F_F^{-1} \int_{\ell_{SO}-\delta}^{\ell_{SO}+\delta} [\Delta G_S^{\text{solv}}(r) + \Sigma_S^{\text{solv}}] r^2 dr = 4 c_S F_O^{-1} \int_{\ell_{SO}-\delta}^{\ell_{SO}+\delta} [\Delta G_O^{\text{solv}}(r) + \Sigma_O^{\text{solv}}] r^2 dr \quad (26)$$

where the identity (26) becomes an indicator of properly normalized experimental first-order differences $\Delta G_O^{\text{solv,norm}}(r)$ and $\Delta G_S^{\text{solv,norm}}(r)$.

In summary, in developing the current interplay we have exposed some frequently overlooked issues and highlighted that the pressing challenge at this juncture is to confront the significant difficulties associated with these null-environment NDIS experiments and translate the proposed novel schemes into versatile tools for the accurate full characterization of oxyanion hydration.

This manuscript has been authored by UT-Battelle, LLC under Contract No. DE-AC05-00OR22725 with the U.S. Department of Energy. The United States Government retains and the publisher, by accepting the article for publication, acknowledges that the United States Government retains a non-exclusive, paid-up, irrevocable, world-wide license to publish or reproduce the published form of this manuscript, or allow others to do so, for United States Government purposes. The Department of Energy will provide public access to these results of federally sponsored research in accordance with the DOE Public Access Plan (http://energy.gov/downloads/doe-public-access-plan).

Acknowledgments: This work was supported by the U.S. Department of Energy, Office of Science, Office of Basic Energy Sciences, Chemical Sciences, Geosciences, and Biosciences Division.

References

[1] B. J. Finlayson-Pitts. *Chem. Rev.* **103**, 4801 (2003).
[2] V. Ramanathan, P. J. Crutzen, J. T. Kiehl, D. Rosenfeld. *Science* **294**, 2119 (2001).
[3] N. Hoshi, M. Kuroda, T. Ogawa, O. Koga, Y. Hori. *Langmuir* **20**, 5066 (2004).
[4] G. A. Ulrich, G. N. Breit, I. M. Cozzarelli, J. M. Suflita. *Env. Sci. Tec.* **37**, 1093 (2003).
[5] A. A. Chialvo, L. Vlcek. *J. Phys. Chem. B* **119**, 519 (2015).
[6] A. A. Chialvo, L. Vlcek. *Fluid Phase Equilib.* **407**, 84 (2016).
[7] R. Caminiti. *J. Chem. Phys.* **84**, 3336 (1986).
[8] R. Caminiti. *Chem. Phys. Lett.* **88**, 103 (1982).
[9] G. Licheri, G. Paschina, G. Piccaluga, G. Pinna. *J. Chem. Phys.* **81**, 6059 (1984).
[10] M. Magini, G. Licheri, G. Paschina, G. Piccaluga, G. Pinna. *X-Ray Diffraction of Ions in Aqueous Solutions: Hydration and Complex Formation*, CRC Press, Inc., Boca Raton (1988).
[11] L. G. Sillén, I. U. o. Pure, A. C. C. o. E. Data, A. E. Martell. *Stability Constants of Metal-ion Complexes [with] Supplement*. Chemical Society (1971).
[12] S. Katayama. *Bull. Chem. Soc. Jpn.* **46**, 106 (1973).
[13] F. H. Fisher, A. P. Fox. *J. Solution Chem.* **8**, 309 (1979).
[14] H. Yokoyama, T. Ohta. *Bull. Chem. Soc. Jpn.* **62**, 345 (1989).
[15] M. Tomsic, M. Bester-Rogac, A. Jamnik, R. Neueder, J. Barthel. *J. Solution Chem.* **31**, 19 (2002).
[16] M. Bester-Rogac, V. Babic, T. M. Perger, R. Neueder, J. Barthel. *J. Mol. Liq.* **118**, 111 (2005).
[17] M. Bester-Rogac. *J. Chem. Eng. Data* **53**, 1355 (2008).
[18] M. Madekufamba, P. R. Tremaine. *J. Chem. Eng. Data* **56**, 889 (2011).
[19] R. Buchner, S. G. Capewell, G. Hefter, P. M. May. *J. Phys. Chem. B* **103**, 1185 (1999).
[20] W. Wachter, S. Fernandez, R. Buchner, G. Hefter. *J. Phys. Chem. B* **111**, 9010 (2007).
[21] R. Buchner, T. Chen, G. Hefter. *J. Phys. Chem. B* **108**, 2365 (2004).
[22] T. Chen, G. Hefter, R. Buchner. *J. Solution Chem.* **34**, 1045 (2005).
[23] G. Hefter. *Pure Appl. Chem.* **78**, 1571 (2006).
[24] D. B. Bechtold, G. Liu, H. W. Dodgen, J. P. Hunt. *J. Phys. Chem.* **82**, 333 (1978).
[25] F. P. Daly, D. R. Kester, C. W. Brown. *J. Phys. Chem.* **76**, 3664 (1972).
[26] A. R. Davis, B. G. Oliver. *J. Phys. Chem.* **77**, 1315 (1973).
[27] F. Rull, C. Balarew, J. L. Alvarez, F. Sobron, A. Rodriguez. *J. Raman Spectrosc.* **25**, 933 (1994).
[28] J. D. Frantz, J. Dubessy, B. O. Mysen. *Chem. Geol.* **116**, 181 (1994).
[29] W. Rudolph, G. Irmer. *J. Solution Chem.* **23**, 663 (1994).
[30] W. W. Rudolph, G. Irmer, G. T. Hefter. *PCCP* **5**, 5253 (2003).

[31] D. Watanabe, H. Hamaguchi. *J. Chem. Phys.* **123**, Article ID 34508 (2005).
[32] E. V. Petrova, M. A. Vorontsova, V. L. Manomenova, L. N. Rashkovich. *Crystallogr. Rep.* **57**, 579 (2012).
[33] W. D. Bale, E. W. Davies, C. B. Monk. *T. Faraday Soc.* **52**, 816 (1956).
[34] R. Nasanen. *Acta Chem. Scand.* **3**, 179 (1949).
[35] H. Yokoyama, H. Yamatera. *Bull. Chem. Soc. Jpn.* **48**, 2719 (1975).
[36] P. A. Bergstrom, J. Lindgren, O. Kristiansson. *J. Phys. Chem.* **95**, 8575 (1991).
[37] J. Stangret, T. Gampe. *J. Phys. Chem. A* **106**, 5393 (2002).
[38] V. S. K. Nair, G. H. Nancollas. *J. Chem. Soc.* Article ID 791, 3934 (1959).
[39] S. Kratsis, G. Hefter, P. M. May. *J. Solution Chem.* **30**, 19 (2001).
[40] C. Akilan, P. M. May, G. Hefter. *J. Solution Chem.* **43**, 885 (2014).
[41] H. Yokoyama, H. Yamatera. *Bull. Chem. Soc. Jpn.* **48**, 2708 (1975).
[42] W. Libus, T. Sadowska, Z. Libus. *J. Solution Chem.* **9**, 341 (1980).
[43] R. Caminiti. *Z. Naturforsch. A* **36**, 1062 (1981).
[44] R. Caminiti, G. Johansson. *Acta Chem. Scand. A* **35**, 373 (1981).
[45] R. Caminiti, G. Paschina. *Chem. Phys. Lett.* **82**, 487 (1981).
[46] G. Licheri, G. Paschina, G. Piccaluga, G. Pinna. *Z. Naturforsch. A* **37**, 1205 (1982).
[47] T. Yamaguchi, O. Lindqvist. *Acta Chem. Scand. A* **36**, 377 (1982).
[48] A. Musinu, G. Paschina, G. Piccaluga, M. Magini. *J. Appl. Crystallogr.* **15**, 621 (1982).
[49] T. Radnai, G. Palinkas, R. Caminiti. *Z. Naturforsch. A* **37**, 1247 (1982).
[50] H. Ohtaki, T. Yamaguchi, M. Maeda. *Bull. Chem. Soc. Jpn.* **49**, 701 (1976).
[51] V. Vchirawongkwin, B. M. Rode, I. Persson. *J. Phys. Chem. B* **111**, 4150 (2007).
[52] J. X. Xu, Y. Fang, C. H. Fang. *Chin. Sci. Bull.* **54**, 2022 (2009).
[53] V. F. Sears. *Neutron News* **3**, 29 (1992).
[54] S. Cummings. *J. Phys. Paris* **45**, 131 (1984).
[55] G. W. Neilson, J. E. Enderby. *J. Phys. Chem.* **100**, 1317 (1996).
[56] I. Howell, G. W. Neilson. *J. Mol. Liq.* **73-4**, 337 (1997).
[57] P. E. Mason, S. Ansell, G. W. Neilson, S. B. Rempe. *J. Phys. Chem. B* **119**, 2003 (2015).
[58] J. E. Enderby. *Chem. Soc. Rev.* **24**, 159 (1995).
[59] G. W. Neilson, P. E. Mason, S. Ramos, D. Sullivan. *Philos. T. Roy. Soc. A* **359**, 1575 (2001).
[60] S. Ansell, A. C. Barnes, P. E. Mason, G. W. Neilson, S. Ramos. *Biophys. Chem.* **124**, 171 (2006).
[61] Y. S. Badyal, A. C. Barnes, G. J. Cuello, J. M. Simonson. *J. Phys. Chem. A* **108**, 11819 (2004).
[62] A. A. Chialvo, J. M. Simonson. *J. Chem. Phys.* **119**, 8052 (2003).
[63] J. L. Fulton, S. M. Heald, Y. S. Badyal, J. M. Simonson. *J. Phys. Chem. A* **107**, 4688 (2003).
[64] T. Megyes, I. Bako, S. Balint, T. Grosz, T. Radnai. *J. Mol. Liq.* **129**, 63 (2006).
[65] H. E. Fischer, J. M. Simonson, J. C. Neuefeind, H. Lemmel, H. Rauch, A. Zeidler, P. S. Salmon. *J. Phys.-Condens. Mat.* **24**, Article ID 505105 (2012).
[66] A. A. Chialvo, J. M. Simonson. *J. Chem. Phys.* **124**, 154509 (2006).
[67] J. E. Enderby, G. W. Neilson. *Rep. Prog. Phys.* **44**, 593 (1981).
[68] D. L. Price, A. Pasquarello. *Phys. Rev. B* **59**, 5 (1999).
[69] A. K. Soper, G. W. Neilson, J. E. Enderby. *J. Phys. C. Solid State* **10**, 1793 (1977).
[70] H. J. C. Berendsen, J. R. Grigera, T. P. Straatsma. *J. Phys. Chem.* **91**, 6269 (1987).
[71] S. L. Wallen, B. J. Palmer, J. L. Fulton. *J. Chem. Phys.* **108**, 4039 (1998).
[72] W. R. Cannon, B. M. Pettitt, J. A. McCammon. *J. Phys. Chem.* **98**, 6225 (1994).
[73] S. Nose. *J. Phys. Soc. Jpn.* **70**, 75 (2001).
[74] H. Okumura, S. G. Itoh, Y. Okamoto. *J. Chem. Phys.* **126**, 084103 (2007).
[75] J. M. Martinez, L. Martinez. *J. Comput. Chem.* **24**, 819 (2003).
[76] D. Fincham. *Mol. Simulat.* **13**, 1 (1994).
[77] A. A. Chialvo, P. T. Cummings. *J. Phys. Chem.* **100**, 1309 (1996).
[78] M. Eigen, K. Tamm. *Z. Elektrochem.* **66**, 93 (1962).
[79] J. C. Poirier, J. H. DeLap. *J. Chem. Phys.* **35**, 213 (1961).
[80] A. A. Chialvo, J. M. Simonson. *Collec. Czech. Chem. Commun.* **75**, 405 (2010).
[81] S. Wasylkiewicz. *Fluid Phase Equilib.* **57**, 277 (1990).